A Sensornet Testbed at the University of Warsaw

Mateusz Michalowski, Przemyslaw Horban, Karol Strzelecki, Jacek Migdal, Maciej Klimek, Piotr Glazar, and Konrad Iwanicki

University of Warsaw, Poland

{mm262512, ph262940, ks249241, jm262954, mk277539, pg262508}
@students.mimuw.edu.pl
{iwanicki}@mimuw.edu.pl

Technical Report TR-DS-01/12
University of Warsaw, July 2012

ABSTRACT

We present a wireless sensor network (sensornet) testbed for routing protocols, which we have deployed at the University of Warsaw. The testbed consists of 100+-sensor nodes dispersed across ten office rooms and supported by additional infrastructure. As we demonstrate through microbenchmarks and experiments with the Collection Tree Protocol (CTP), the testbed constitutes a challenging environment for routing protocols. First, it has a large diameter: from six to nine hops, depending on the radio output power. Second, it offers a highly nonuniform node density: from a few to nearly fifty neighbors. Third, it exhibits a large fraction of asymmetric links.

Faculty of Mathematics, Informatics and Mechanics
University of Warsaw
ul. Banacha 2
02-097 Warszawa
Poland

Contents

1 Introduction

In this technical report, we introduce a 100+-node wireless sensor network (sensornet) testbed that we have built at the University of Warsaw. The testbed is designed to be a conclusive and challenging environment for experiments with routing protocols. More specifically, it emphasizes the following three features:

Large diameter
The larger the number of hops that a routing protocol has to perform to deliver a packet between nodes, the more work there is for the protocol.

Nonuniform density
The larger the differences in the number of neighbors between different nodes, the more challenging it is for a routing protocol to maintain local routing state at each node.

Asymmetric links
The more asymmetric wireless links are, the more difficult it is for a routing protocol to provide reliable routing paths.

We present the physical organization, as well as the hardware and software of the testbed. We also experimentally validate how the testbed fulfills the three aforementioned design objectives. More specifically, we show that (1) depending on the radio output power, the diameter of the testbed is from six to nine hops, (2) a node can have from a few to nearly fifty neighbors, and (3) more than 15% of links are asymmetric. Overall, the testbed indeed constitutes a challenging platform for sensornet routing protocols.

The rest of the report is organized as follows. Section 2 starts with presenting the architecture of the testbed. Section 3 studies the aforementioned connectivity properties of the testbed through microbenchmark experiments. Section 4 presents the performance of a complete all-to-one routing protocol, Collection Tree Protocol (CTP). Finally, Section 5 concludes. More detailed information on the testbed can be found in [8].

2 Architecture

The testbed consists of 102 permanent wireless sensor nodes located in ten office rooms and supported by and additional wired hardware-software infrastructure.

2.1 Nodes

The nodes belong to the SOWNet Technologies' G-Node G301 family [9] (see Fig. 1 and Table 1). Each comes with a USB interface that can be used for programming, debugging and data logging. This simplifies reprogramming, and minimizes the disruption to wireless communication during experiment monitoring. Moreover, as a node is powered from the USB connection, no regular battery replacements are necessary.

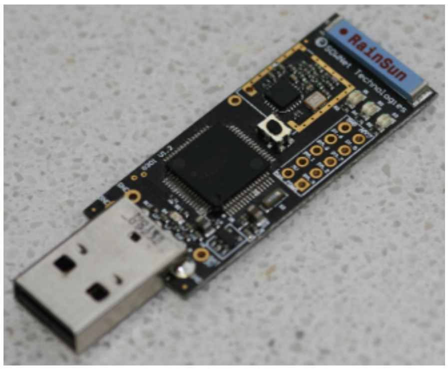

Fig. 1. G-Node G301 (housing disassembled)

Microcontroller family	TI MSP430
Radio chip	TI CC1101
CPU speed	1 – 16MHz
RAM size	8KB
ROM size	116KB
Radio band	868MHz
Radio throughput	250kbit/s
Indoor radio range	10 – 20m
Outdoor radio range	30m
Dimensions	60 x 6 x 19mm

Table 1. Selected G-Node G301 parameters

G301 supports TinyOS 2.1 [7], which provides an abstraction layer over node hardware components. Applications running on the nodes can be written in the nesC programming language [2]. As a result, a programmer can focus on the implementation of a routing protocol and, to some extent, ignore hardware-specific aspects.

2.2 Localization

The testbed is located on the third floor of the north wing of the Mathematics, Informatics and Mechanics faculty building (see Fig. 2). The nodes are distributed among ten rooms on both sides of the corridor.

In each room, there are from 8 to 11 nodes, the most of which are hidden away from humans. Not only does this approach minimize the nodes' negative aesthetic impact, but also reduces the risk of accidentally damaging the installation. Despite being hidden, the node locations are still diverse: the nodes are installed at different heights, on various surfaces (e.g., wood, carpet, concrete, stone), and with different distances and orientations with respect to each other.

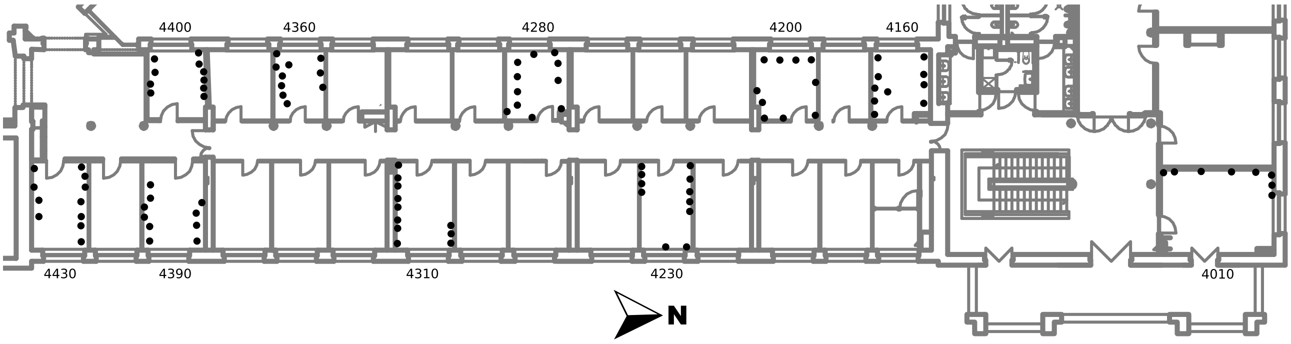

Fig. 2. Node placement

2.3 Infrastructure

To make use of the USB interface of G301, additional hardware is installed in each room. The central point of each room's infrastructure is an Asus EeeBox EB1021 mini PC, to which sensor nodes are connected via USB. We decided to use one mini PC per room, considering both the price of EB1021 and the limitations of USB topologies. For external communication, mini PCs are connected to a LAN. Each mini PC is responsible for programming the connected nodes, monitoring their status, and providing wired bidirectional communication.

To keep control over the 10 mini PCs and 102 nodes dispersed across the building, a dedicated management platform has been developed and deployed on a separate powerful Linux server. In this report, we omit the details of the platform for brevity. For more information, please, refer to [8].

3 General Properties

We evaluate basic connectivity properties of the testbed with a simple TinyOS application, which we developed for our previous testbed, KonTest [5]. In short, at a random moment in every minute, each node running the application broadcasts a 40-byte radio packet. Likewise, upon reception of a similar packet from another node, the receiver logs the packet's metadata, such as a sequence number, received signal strength indicator (RSSI), and link quality indicator (LQI). Based on the metadata logged by all nodes, we compute packet reception ratios (the fraction of successfully delivered packets) for wireless links, and correlate these values with the physical signal quality indicators: RSSI and LQI. The link qualities measured in this way should reflect the actual link qualities well, because the long (one-minute) inter-packet intervals essentially eliminate packet collisions.

We ran the application on all 102 nodes with 5 different radio output power levels (i.e., 12dBm, 10dBm, 7dBm, 5dBm, 0dBm). For any given power level, the run took at least a few days to deliver long-term link quality information and to maximize our confidence in the results.

3.1 Link grades

In subsequent sections, we use so-called link grades to classify the quality (measured as packet reception rate) of wireless links between nodes (see Table 2). Note that link quality normally refers to a one-way link from a sender to a receiver (so-called unidirectional link quality). However, in real applications a packet sent by a node is often required to be acknowledged by the receiver. Therefore, it reasonable to also introduce so-called bidirectional link quality. We define the bidirectional quality of a link as a product of unidirectional qualities of the link in both directions.

Grade	Range	Description
A	(0.9, 1]	reliable uni-/bi-directional links
B	(0.5, 0.9]	utilizable uni-/bi-directional links
C	(0, 0.5]	poor uni-/bi-directional links
R	(0.81, 1]	reliable bidirectional routing links

Table 2. Link grades

3.2 Network connectivity

3.2.1 Packet reception rate

To illustrate the quality of radio links between each pair of nodes, Fig. 3, Fig. 4, and Fig. 5 depict connectivity maps for different radio output power levels. Each line in the figures represents the packet reception rate of a bidirectional link between two nodes. The darker is the line, the higher the packet reception rate it represents, and thus, the more reliable the corresponding link.

In general for all analyzed radio power levels, the network is connected. However, for the power level of 0dBm,

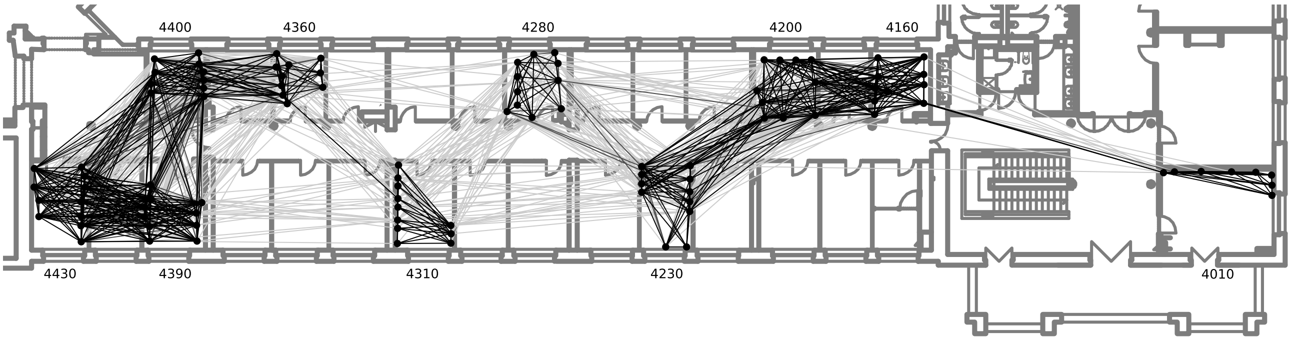

Fig. 3. Connectivity map (0dBm)

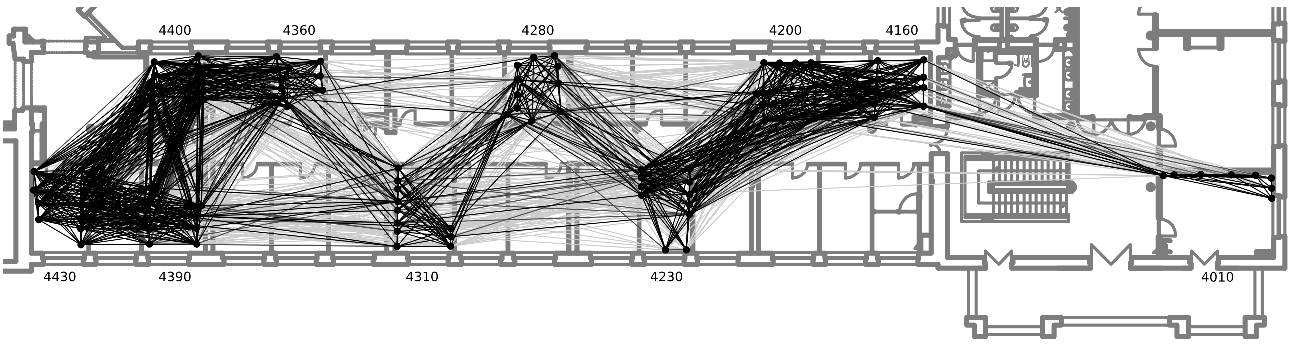

Fig. 4. Connectivity map (7dBm)

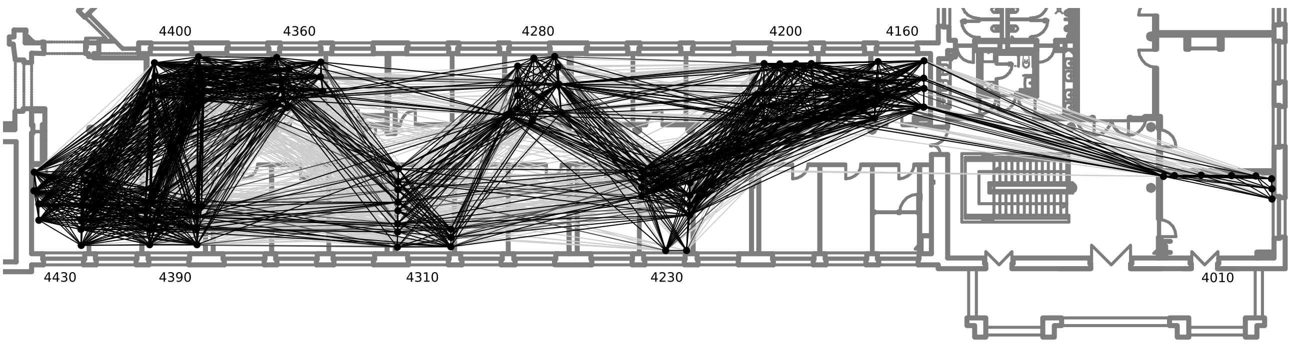

Fig. 5. Connectivity map (12dBm)

a lack of network partitions is achievable only when all-grade links are considered. In contrast, when analyzing the connectivity graph induced only by A- and B-grade links, the graph appears to be split in two parts (with the line of the split located between rooms 4310 and 4280). The most of A-grade links, connect nodes located in the same room or in neighboring rooms.

The power level of 7dBm is the lowest that offers a connected network based solely on bidirectional A-grade links. A lot of C-grade links that are available for the 0dBm power level become B- or even A-grade with the 7dBm power level. Moreover, a number of new C-grade links become available and connect more distant areas of the testbed. As an example, direct connectivity between rooms 4360 and 4230 is possible with a few C-grade links.

The highest power level of 12dBm introduces a lot of new A-grade links between more distant room pairs like 4360 and 4280, while for the 7dBm these are connected mostly with B-grade links. However, the connections to room 4010 are still available mostly from the closest room, 4160.

In general, although link qualities increase for higher radio power levels and lower inter-node distances, there are some exceptions from this rule, especially when C-grade links are considered. For example, a few C-grade links between rooms 4230 and 4010 disappear after increasing the power level: the power level of 10dBm offers 7 such links, but for the highest power level, 6 of those links no longer exist. Likewise, obstacles, such as walls and furniture, influence link quality. This is especially visible when considering the 0dBm case (see Fig. 3). As an example, the

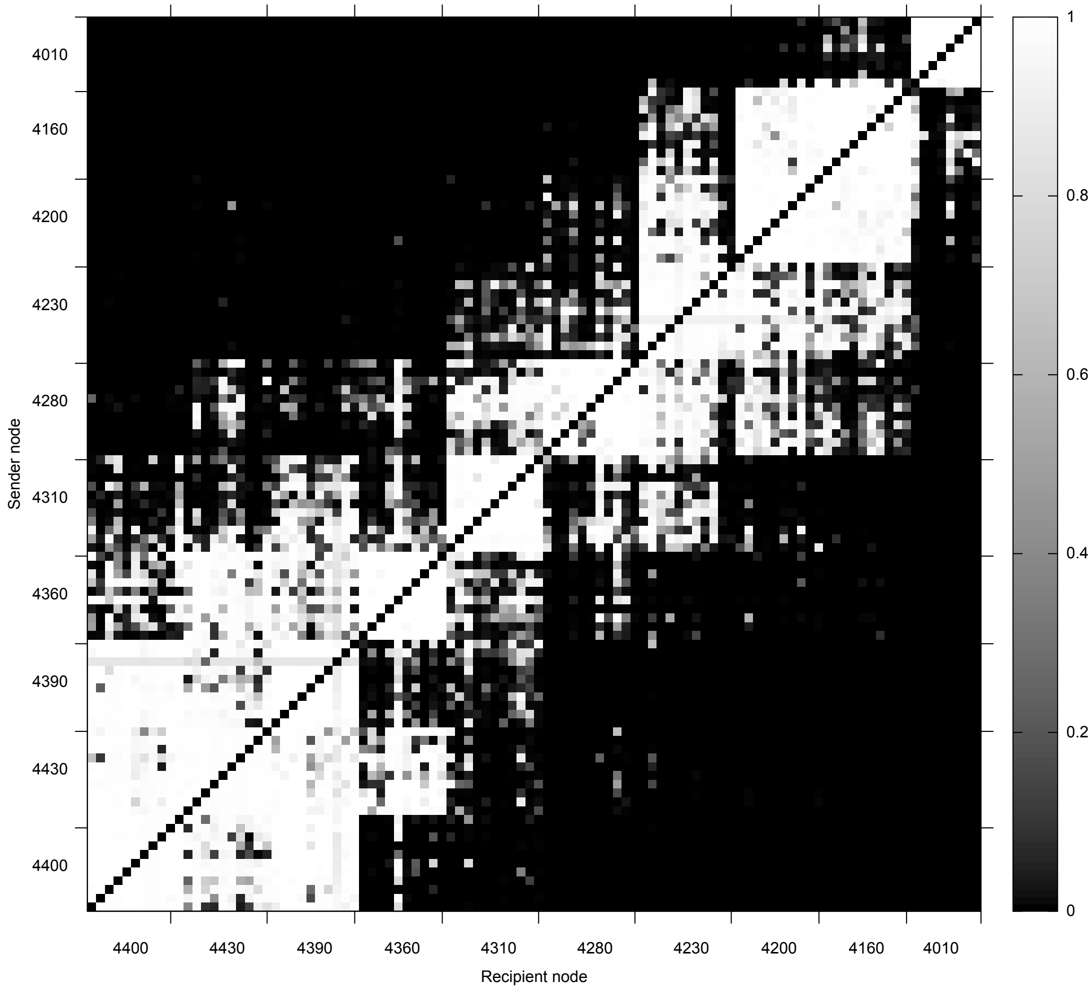

Fig. 6. Reception rate in 10-room experiment (7dBm)

right bottom corner of room 4280 in the figure corresponds to a thicker wall. The quality of the links around this spot is significantly higher than that of the links going directly through the spot. Links between rooms 4010 and 4160 also illustrate the influence of obstacles. As there is mostly open space between these rooms, the links have noticeably higher quality than an average link over a similar distance.

Finally, Fig. 6 visualizes the connectivity map for the radio power level of 7dBm (from Fig. 4) in the form of connectivity matrix. We can observe that radio links between nodes in one room are typically reliable and form cliques. In contrast, links between rooms seem more random. Essentially, the matrix indicates that the testbed fulfills the three design goals: it has a large diameter, nonuniform neighborhood sizes, and many asymmetric links. We confirm these properties further in this report.

3.2.2 Physical quality indicators

As RSSI and LQI measure the quality of the received radio signal, we analyze their relevance in estimating link quality. Figure 7 illustrates for each link the correlation between the packet reception rate for the link and the RSSI values of packets received over the link. One point in the figure represents the RSSI of a single packet.

In general, RSSI values are increasing for links with higher reception rates. RSSI values above -75dBm indicate a reliable link (with a high packet reception rate). In contrast, values below -85dBm give a strong suggestion that the link may not be stable. As the variance of RSSI is quite noticeable, the values in-between can be measured for links with many different reception rates. However, when a given link is considered, the variance of RSSI is relatively small. Overall, there is correlation between RSSI and packet reception rates that can be exploited by routing protocols, which is consistent with prior work [10].

Figure 8 depicts analogous results for the LQI metric. The figure shows that for higher reception rates, the average LQI values are decreasing slightly, which is consistent with the specification of the CC1101 radio employed by G301 [9]. However, since the links with the lowest reception rates can display virtually any LQI, it is hardly possible

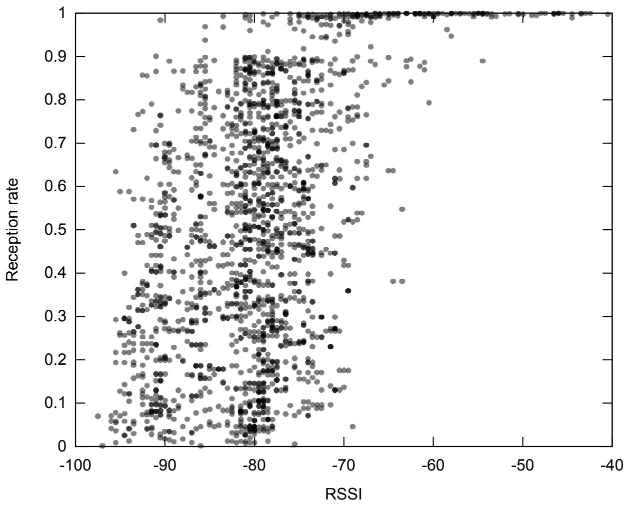

Fig. 7. RSSI correlated with packet reception rate

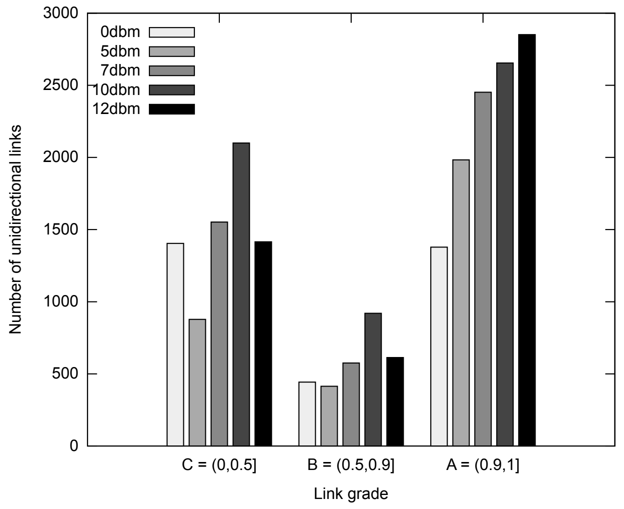

Fig. 9. Distribution of unidirectional link qualities

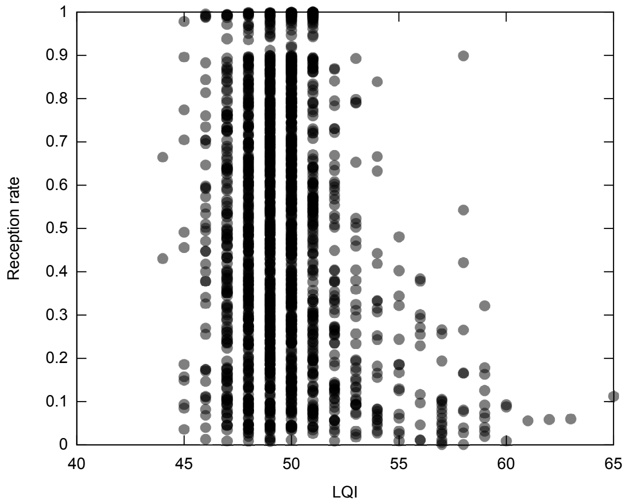

Fig. 8. LQI correlated with packet reception rate

to estimate the reception rate based solely on LQI values. Therefore, at least in the case of G301, the LQI metric is less useful for identifying high-quality links for routing protocols than RSSI.

3.2.3 Distribution of link qualities

For a routing protocol, not only the quality, but also the quantity of links is important. In particular, if high-quality links constitute a significant fraction of all links, it is easier for a routing protocol to identify them. The distribution of unidirectional link qualities (grouped into the aforementioned grades) is shown in Fig. 9.

The figure illustrates that the link qualities have a bimodal-like distribution: most of the links fall into either the worst, C-grade category, or the best, A-grade category; in contrast, there are few B-grade links. Furthermore, although increasing the radio output power usually increases the total number of links, there are exceptions from this rule.

First, when comparing the 0dBm case with the 5dBm case, one can observe that the link grade distribution changes noticeably. However, the overall number of links in the network remains almost the same. Analyzing connectivity maps for these output powers, we can notice that although some links increase their grade at 5dBm, hardly any new links are introduced, as the stronger signal is still too weak to reach extra nodes at higher distances. In effect, the number of A-grade links increases significantly, but the overall link count remains almost unchanged.

Second, the overall link count drops by almost 800 when comparing the 12dBm radio output power to the 10dBm power. More specifically, there are almost 700 fewer C-grade links and about 300 fewer B-grade links, while, at the same time, the number of A-grade links increases by only about 200. This phenomenon may be caused by multi-path effects affecting low-quality links.

An analogous distribution of bidirectional link grades is presented in Fig. 10. It is similar to the unidirectional one. What is worth noticing, though, is the fact that the total number of bidirectional links is lower than the half of the unidirectional links. This difference is caused by link asymmetry: a nonexistent unidirectional link precludes the existence of the corresponding bidirectional link, even if the link in the reverse direction has a high quality.

3.3 Diameter

Having discussed the basic connectivity properties of the testbed, let us proceed to assessing how the testbed fulfills the three design goals we formulated initially. Our first goal was a large diameter, measured as the maximal number of hops a packet has to take to reach its destination node over a shortest path. A large diameter stresses a routing protocol in many aspects: the amount of state maintained by each node,

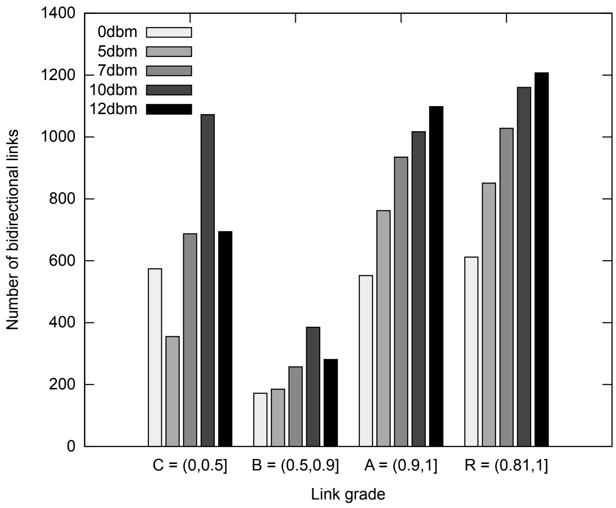

Fig. 10. Distribution of bidirectional link qualities

the dilation of routing paths, and the latency of reacting to changes in the network, to name just a few examples [6]. Figure 11) presents how many hops are necessary to deliver a packet between each pair of nodes over A-grade-only unidirectional (outgoing) links.

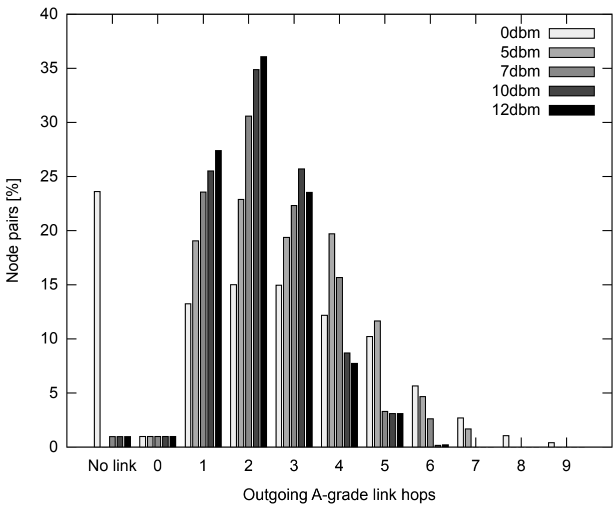

Fig. 11. Routing paths over outgoing A-grade links

For the 0dBm radio output power, no communication over A-grade-only links is possible for almost 25% of node pairs because of the low number of A-grade links at this power level. For the 5dBm power, this is no longer the case: all node pairs are able to communicate over A-grade links. However, when considering the power levels above 5dBm, again no communication is possible for about 1% of node pairs. This phenomenon is due to one node whose all outgoing links are graded below A at power levels greater than 5dBm. This again can likely be attributed to multi-path effects of radio signal.

For all power levels, the most common distance between a node pair is 2 hops. Importantly, however, the maximal inter-node distance (the network diameter) is 6 hops for the two highest radio output power levels. Moreover, for lower power levels, the diameter further grows. For the 5dBm case, it is 7 hops, while for the power of 0dBm, it is as large as 9 hops. In other words, the diameter of the testbed is relatively large compared to other testbeds deployed to date [4].

Figure 12 illustrates analogous results for bidirectional R-grade links. For the radio power level of 0dBm, communication is not possible between almost 60% of node pairs. In contrast, for all higher power levels, communication is possible for all node pairs. Similarly to the unidirectional case, 2 hops is the the most common distance. The diameter, in turn, varies between 5 hops for the 12dBm radio power level, and 8 hops for the 5dBm power. To sum up, the testbed has indeed a relatively large diameter.

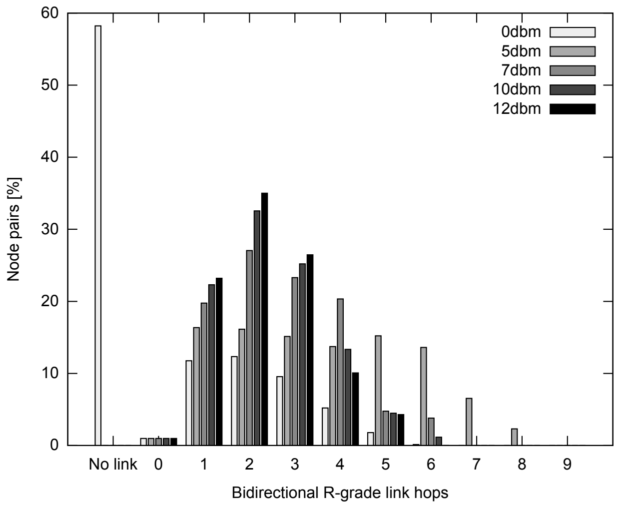

Fig. 12. Routing paths over bidirectional R-grade links

3.4 Neighborhood size

Many routing protocols require nodes to store information about high-quality links to other nodes in the radio range (neighbors). If the number of neighbors varies significantly between nodes, a routing protocol may have difficulties discriminating high-quality links from low-quality ones without significantly overprovisioning memory for neighbor entries. Moreover, retransmission strategies that improve packet delivery in dense areas may fail in sparser areas of the network, thereby degrading end-to-end packet delivery rates. For these reasons, nonuniform neighborhood size distribution was our second design goal for the testbed.

Figure 13, Fig. 14, and Fig. 15 present the distribution of the number of neighbors for the 7dBm radio output power and outgoing, incoming, and bidirectional links, respectively. When outgoing neighbors are considered, it can be concluded that the results are concentrated around an average value of 28 neighbors. The peak for the degree of 7 is achieved for nodes in room 4010, which are slightly separated from the rest of the network. This phenomenon is less pronounced for the incoming neighbors, as the variation of the values is significantly higher than for the outgoing neighbors. In other words, there are areas of the testbed that are quite dense, with a few tens of neighbors per node, as well as areas that are extremely sparse, with just a few neighbors per node.

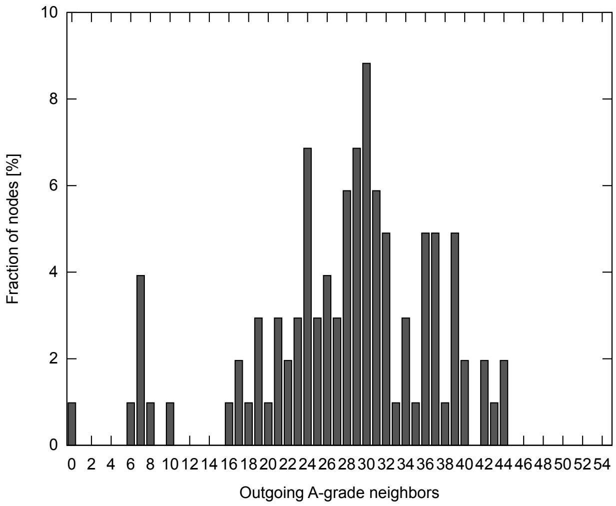

Fig. 13. Outgoing A-grade neighbor distribution

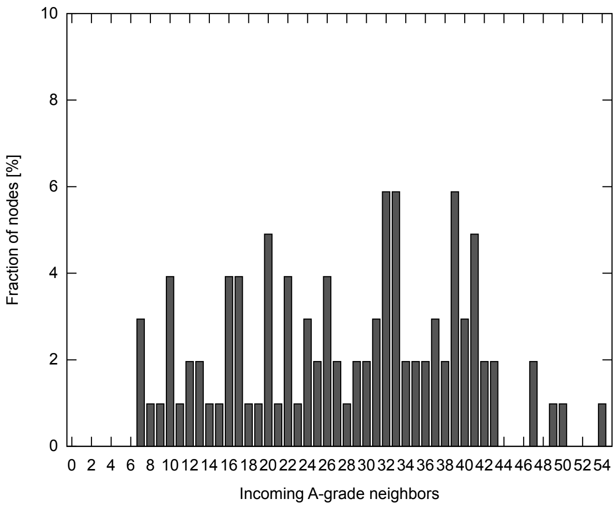

Fig. 14. Incoming A-grade neighbor distribution

Figure 17 shows that the situation does not change for the other power levels. Even though the higher the power level is, the more neighbors each node has, the variance in the number of neighbors remains high for all considered power levels. Overall, the testbed fulfills the goal of highly nonuniform neighborhood sizes.

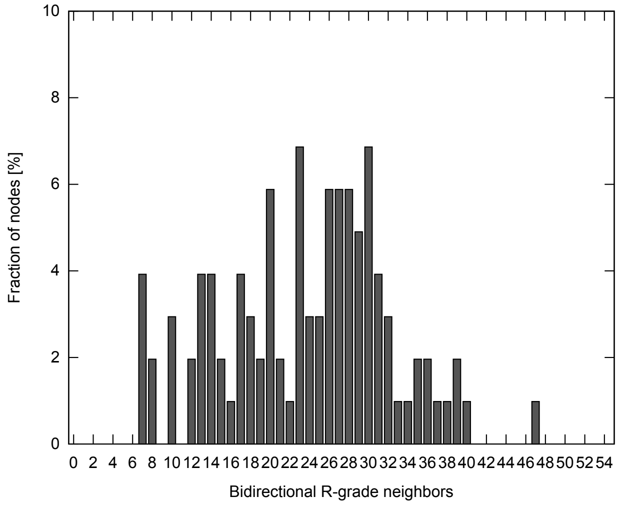

Fig. 15. Bidirectional R-grade neighbor distribution

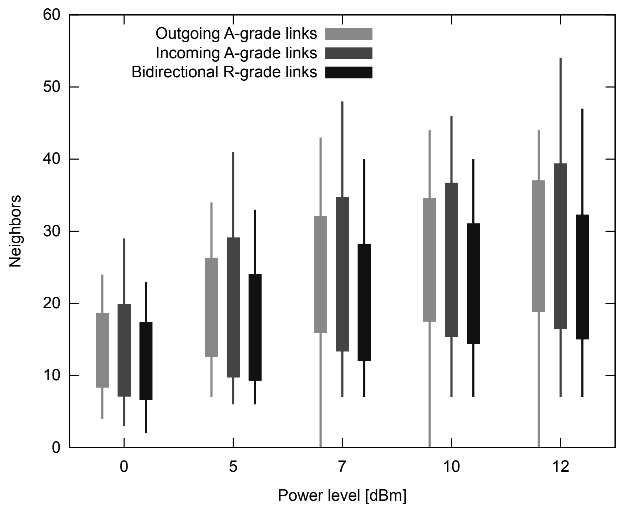

Fig. 17. Neighbor distribution for different radio power

3.5 Link asymmetry

The last design goal of our testbed were numerous asymmetric links. Such links are particularly challenging for routing protocols. First, a node may classify a link as a high-quality one based solely on the incoming packet reception rate [1]. If the link is asymmetric, the node will not be able to reliably send any packet over it. Second, if in contrast the outgoing packet reception rate is high, but the incoming one is low, a protocol that requires hop-by-hop acknowledgments for packet forwarding will not be able to utilize the link.

To analyze the properties of asymmetric links, we compare all A-grade unidirectional links with their corresponding reverse links. Asymmetric links are then classified based on the relative difference between their reception rates in both directions into the following three categories: A_{35}, A_{65} and A_{95} (see Table 3). The fractions of links in each of these

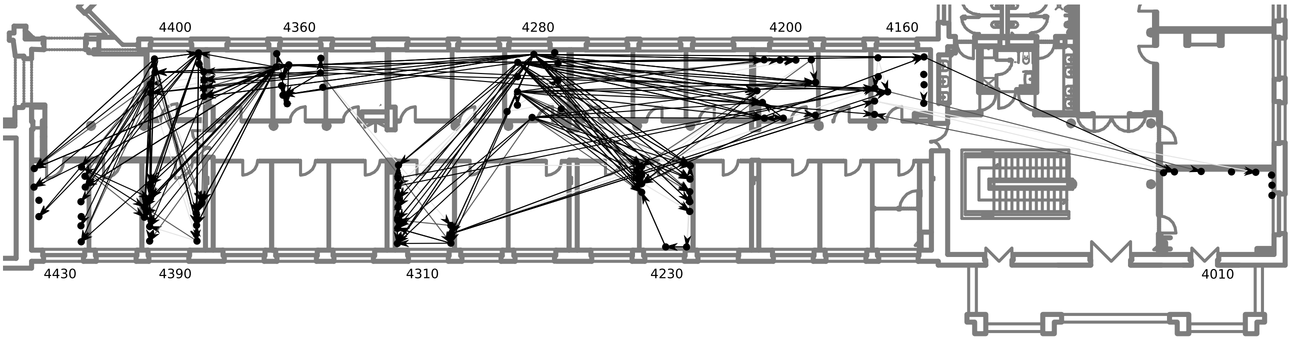

Fig. 16. Link asymmetry map (7dBm)

asymmetry categories are presented in Fig. 18.

Grade	Asymmetry level
A_{35}	(35%, 65%]
A_{65}	(65%, 95%]
A_{95}	(95%, 100%]

Table 3. Link asymmetry categories

For the radio output power levels of 0dBm and 10dBm, all asymmetry categories cover a similar fraction of A-grade links. This results in the overall fraction of asymmetric links of 15% and 20%, respectively. However, for the remaining power levels, a large number of links are classified in the A_{95} asymmetry category. As an example, 15% of A-grade links at the 5dBm output power correspond to reverse links with the reception rate lower than 0.05. This means that if a link is asymmetric, the extent of this asymmetry is very large with a high probability.

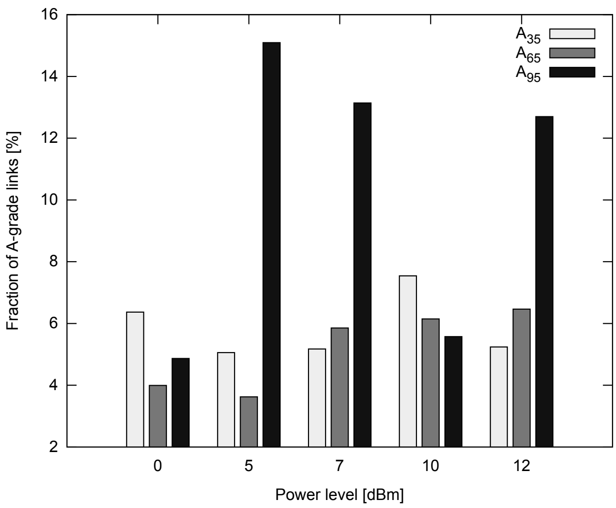

Fig. 18. Asymmetry of A-grade links

Figure 16 shows which nodes have asymmetric links. In the figure, each node pair with an asymmetric link is connected by an arrow, which indicates the direction of the high-quality link. The darker is the arrow, the more significant the asymmetry it illustrates.

The figure suggest that asymmetric links usually connect distant nodes. In particular, at the power level of 7dBm almost all such links connect different rooms. To sum up, for any power level at least 15% of links are asymmetric, and, moreover, the extent of the asymmetry is high. In other words, the testbed fulfills also our last design goal.

4 Collection Routing

In addition to the previous microbenchmarks, we present experiments with a complete routing protocol in order to illustrate how such a protocol can perform on the testbed. To this end, we employ the well-known Collection Tree Protocol (CTP) [3].

CTP is an all-to-one routing protocol: all packets from the network are routed to a single or at most a few sink nodes. To perform routing, CTP maintains a spanning tree rooted at the sink node. Each node simply forwards all incoming packets to its parent node in the tree. To construct and maintain the tree, in turn, each node periodically broadcasts a so-called beacon packet. In this way, based on the received beacon packets, every node can select its parent in the tree. The details can be found in the original description of CTP [3].

4.1 Experimental settings

CTP is utilized, among others, by the TestNetwork application, which belongs to the standard TinyOS 2.1 distribution. Each node programmed with the TestNetwork application periodically creates a packet, which is subsequently routed by the network to the closest sink. When the packet is received by the sink node, it is forwarded to a PC to which the sink node is attached over the USB interface.

We ran the TestNetwork application with three different single-sink configurations, which are marked as L, M, and R in Fig. 19. During the experiments we experienced a long-lasting failure of the testbed infrastructure in room 4400. Six nodes that did not take part in the experiment are

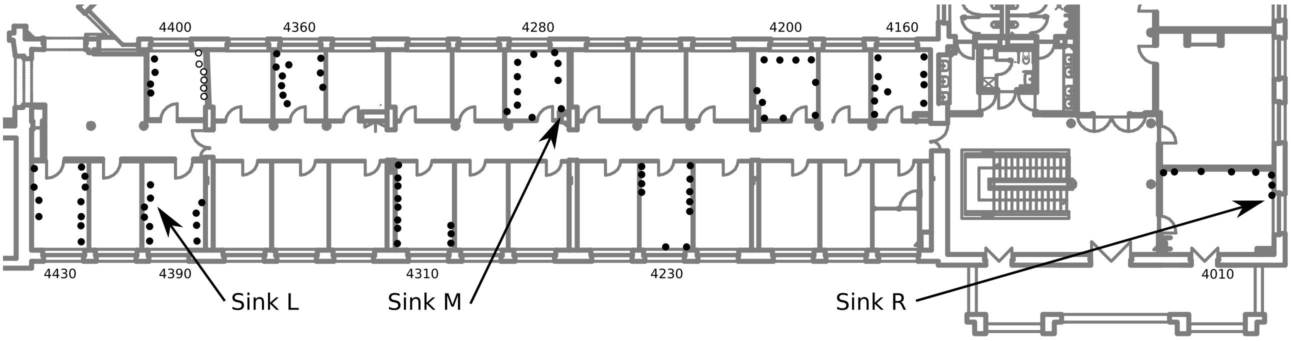

Fig. 19. Sink node layout in CTP experiments

Parameter	Used by	Description	Values used
Packet interval	TestNetwork	The interval between packets sent by a node is selected randomly. This parameter limits the maximal value of the interval. Its value prevents the network from overloading a sink node and minimizes packet collisions.	5min
Sink nodes	TestNetwork	The identifier of the sink node. We used one sink per experiment.	L, M, R
Number of retransmissions	CTP	The maximal number of retransmissions of a packet performed by a node at each hop. After exceeding this value, the node drops the packet.	30
White bit function	CTP	This function indicates a physical channel quality and is used by CTP's Four-Bit Wireless Link Estimator [1]. For each received packet, the function returns the estimator's white bit. A set white bit implies that during the reception, the quality of the signal is high.	$RSSI \geq -80$
Max neighborhood size	CTP	CTP (actually the Four-Bit Wireless Link Estimator) maintains a list of neighbors from which an alternative parent may be chosen. The size of this list is limited by this parameter.	10
Radio output power	G-Node	The strength of the outgoing radio signal of each node.	5dBm

Table 4. CTP experimental settings

Test	Sink	Undelivered	Hops	Cost	UP	PCR	Beacons
T_L	L	0%	4.75	4.99	4.17	2.9%	84.5%
T_M	M	0%	2.34	2.44	1.22	0.2%	60.7%
T_R	R	1.1%	7.23	7.41	1.08	0.2%	60.6%

Table 5. CTP performance summary

marked with white circles in Fig. 19. Table 4 describes the parameters used in the tests. The parameters have mostly default values.

4.2 Experimental metrics

We are interested in the standard CTP metrics:

Fraction of undelivered packets
The fraction of packets created by the test application that are undelivered to the sink.

Hop count
The average number of hops required to deliver a packet to the sink.

Cost
The number of transmissions for each delivered packet. Ideally, this value should be equal to the number of hops the packet travels. However, retransmissions may occur during the delivery of the packet.

Unique parents per node (UP)
The average number of unique parents that a node has during a test.

Parent change rate (PCR)
This value indicates how large the number of parent changes is compared to the number of packets created by a node.

Beaconing rate

Beacon rate compares the number of beacons broadcast by CTP to maintain the routing tree to the number of data packets created by the TestNetwork application.

For each test, all the metrics are calculated based on experimental data collected at least 1h after the start of the test. Such a delay is enough for CTP to fully bootstrap a stable routing tree.

4.3 Experimental results

Table 5 summarizes the values of these metrics in the conducted experiments. Let us start with the packet delivery rates. For both L and M sink nodes, CTP offers almost 100% packet delivery. On the routes to sink node R, in turn, approximately 1% of packets are dropped. The higher value for node R is likely due to longer routing paths (see below). Essentially, the longer a routing path is, the more places something may go wrong with the packet, and thus, the higher the chance that the packet will not be delivered to the sink.

The lengths of routing paths are correlated closely with the placement of a sink node in the network. Sink nodes at the edges of the network or in sparser areas require longer routing paths. More specifically, for sink node M, which is in the center of the network, only 2.34 routing hops are required on average. Node L, which is at the edge, but also in a dense region, requires 4.75 hops on average. Finally, node R which is not only at the edge, but also in a sparse area, is the most demanding in terms of routing: it requires 7.23 hops on average.

The cost of packet delivery is relatively low in all cases, as approximately only 5% of packet transmissions are repeated. This indicates that CTP is effective in identifying high-quality links.

When it comes to the stability of the routing topology, sink node L offers the least stable tree in terms of the parent change rate. With this node as the sink, a node has 4.17 unique parents on average, whereas for the other sink nodes, the number of unique parents is close to 1. The large number of unique parents is best explained by comparing Fig. 20 and Fig. 21, which present the links used by CTP for sink node L and sink node M, respectively. The darker is the line, the more packets are transferred over the corresponding link. For sink node L, in room 4200, there are a lot of light-gray links, which indicates a large number of unique parents. In general, the more equally good (i.e., equally distant from the sink) parent candidates a node has, the more likely the node is to change its parent, which is exactly the case for room 4200 in Fig. 20.

Finally, the parent change rate of a node is related to the number of unique parents the node has. For the least stable topology, the one with sink node L, the average parent change rate is only 2.9%. This means that CTP does not waste a lot of traffic into reorganizing its routing topology.

To sum up, despite the challenging properties of the testbed, CTP performs well. It is thus a good starting point for research on routing. There are, however, some areas, such as parent changes, exploring which can potentially lead to new improvements of routing algorithms.

5 Conclusion

We presented our testbed, designed specifically for experimenting with routing protocols. The testbed consists of 100+-sensor nodes dispersed across ten office rooms and supported by additional infrastructure. As we demonstrated with microbenchmarks and experiments CTP, the testbed constitutes a challenging environment for routing protocols. First, it has a large diameter: from six to nine hops, depending on the radio output power. Second, it offers a highly nonuniform node density: from a few to nearly fifty neighbors. Third, it exhibits a large fraction of asymmetric links. We thus believe that the testbed will be an important experimental environment in our future research activities.

Acknowledgment

The research presented in this report as well as the hardware for the testbed were supported by the Foundation for Polish Science under grant HOMING PLUS/2010-2/4, cofinanced from the Regional Development Fund of the European Union within the Innovative Economy Operational Program, and a START scholarship (K. Iwanicki).

References

[1] Fonseca, R., Gnawali, O., Jamieson, K., and Levis, P. Four-Bit Wireless Link Estimation. In *Sixth Workshop on Hot Topics in Networks (HotNets)* (Nov. 2007).

[2] Gay, D., Levis, P., von Behren, R., Welsh, M., Brewer, E., and Culler, D. The nesC language: A holistic approach to networked embedded systems. *SIGPLAN Not. 38*, 5 (May 2003), 1–11.

[3] Gnawali, O., Fonseca, R., Jamieson, K., Moss, D., and Levis, P. Collection Tree Protocol. In *Proceedings of the 7th ACM Conference on Embedded Networked Sensor Systems (SenSys'09)* (November 2009).

[4] Iwanicki, K., and Azim, T. Experimentally studying the sensornet point-to-point routing techniques spectrum. In *INSS'10: Proceedings of the 7th IEEE International Conference on Networked Sensing Systems* (Kassel, Germany, June 2010), pp. 6–13.

[5] Iwanicki, K., Gaba, A., and van Steen, M. KonTest: A wireless sensor network testbed at Vrije Universiteit Amsterdam. Tech. Rep. IR-CS-045, Vrije Universiteit Amsterdam, Amsterdam, the Netherlands, August 2008.

[6] Iwanicki, K., and van Steen, M. On hierarchical routing in wireless sensor networks. In *IPSN'09: Proceedings of the 8th ACM/IEEE International Conference on Information Processing in Sensor Networks, IP Track* (San Francisco, CA, USA, April 2009), pp. 133–144.

[7] Levis, P., Madden, S., Polastre, J., Szewczyk, R., Whitehouse, K., Woo, A., Gay, D., Hill, J., Welsh, M., Brewer, E., and Culler, D. TinyOS: An Operating System for Sensor

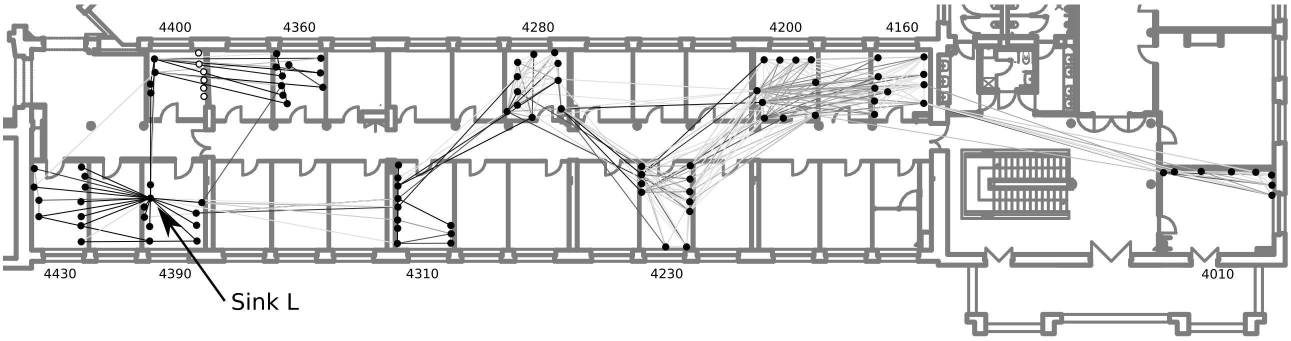

Fig. 20. Up-links used by CTP for sink node L

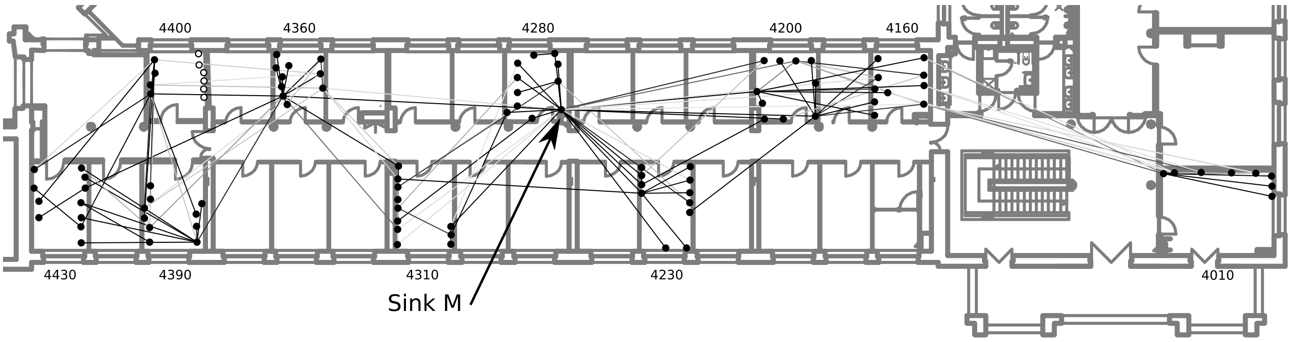

Fig. 21. Up-links used by CTP for sink node M

Networks Ambient Intelligence. In *Ambient Intelligence*, W. Weber, J. M. Rabaey, and E. Aarts, Eds. Springer Berlin Heidelberg, Berlin/Heidelberg, 2005, ch. 7, pp. 115–148.

[8] MICHALOWSKI, M. An experimental platform for wireless sensor networks. Master's thesis, University of Warsaw, June 2012.

[9] SOWNET TECHNOLOGIES B.V. G-Node G301. `http://www.sownet.nl/download/G301Web.pdf`.

[10] SRINIVASAN, K., AND LEVIS, P. RSSI is under appreciated. In *EmNets'06: Proceedings of the 3rd Workshop on Embedded Networked Sensors* (Cambridge, MA, USA, 2006).